

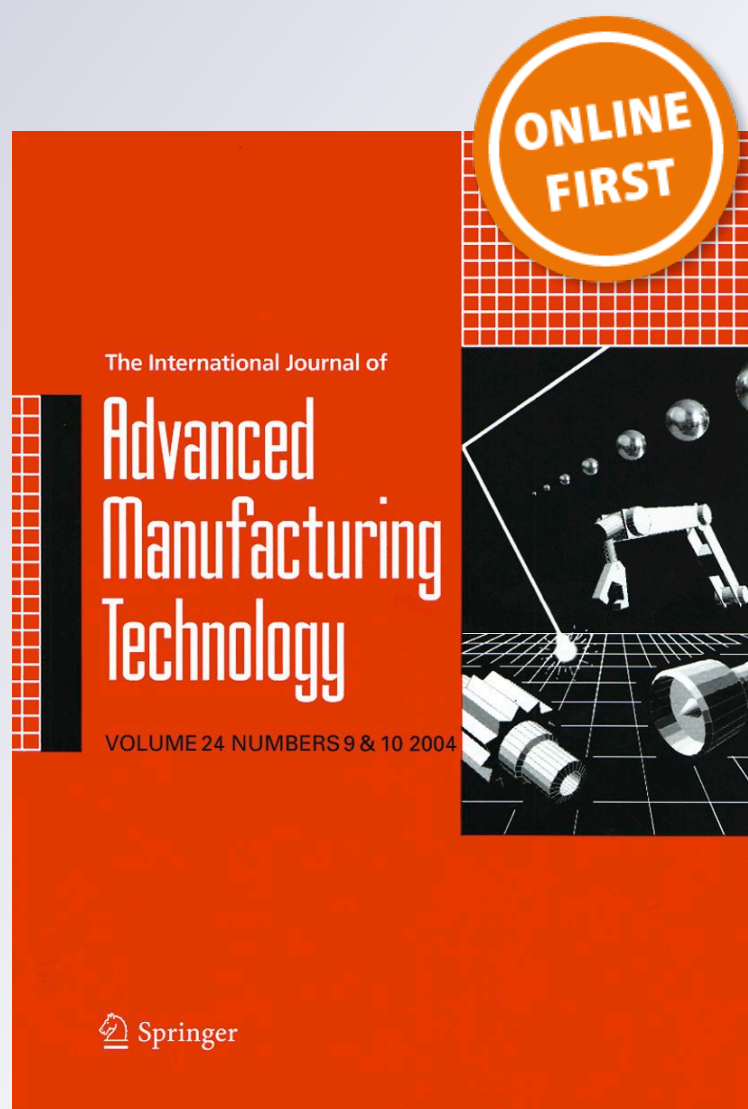
Improving precision in the prediction of laser texturing and surface interference of 316L assessed by neural network and adaptive neuro-fuzzy inference models

H. Sohrabpoor, R. Taherzadeh Mousavian, M. Obeidi, I. U. Ahad & D. Brabazon

**The International Journal of
Advanced Manufacturing Technology**

ISSN 0268-3768

Int J Adv Manuf Technol
DOI 10.1007/s00170-019-04291-z



Your article is protected by copyright and all rights are held exclusively by Springer-Verlag London Ltd., part of Springer Nature. This e-offprint is for personal use only and shall not be self-archived in electronic repositories. If you wish to self-archive your article, please use the accepted manuscript version for posting on your own website. You may further deposit the accepted manuscript version in any repository, provided it is only made publicly available 12 months after official publication or later and provided acknowledgement is given to the original source of publication and a link is inserted to the published article on Springer's website. The link must be accompanied by the following text: "The final publication is available at link.springer.com".



Improving precision in the prediction of laser texturing and surface interference of 316L assessed by neural network and adaptive neuro-fuzzy inference models

H. Sohrabpoor^{1,2} · R. Taherzadeh Mousavian^{1,2} · M. Obeidi^{1,2} · I. U. Ahad^{1,2} · D. Brabazon^{1,2}

Received: 2 March 2019 / Accepted: 9 August 2019
 © Springer-Verlag London Ltd., part of Springer Nature 2019

Abstract

Laser-based surface texturing provides highly controlled interference fit between two parts. In this work, artificial intelligence-based models were used to predict the surface properties of laser processed stainless steel 316 samples. Artificial neural network (ANN) and adaptive neuro-fuzzy inference system (ANFIS) were used to predict the characteristics of laser surface texturing. The models based on feedforward neural network (FFNN) were developed to examine the effect of the laser process parameters for surface texturing on 316L cylindrical pins. The accuracy of the models was measured by calculating the root mean square error and mean absolute error. The reliability of the ANFIS and FFNN models for the output prediction of the laser surface texturing (LST) system were investigated by using the data measured from experiments based on a 3³ factorial design, with main processing parameters set as laser power, pulse repetition frequency, and percentage of laser spot overlap. The relative assessment of the models was performed by comparing percentage error prediction. Finally, the impact of input data was examined using predicted response surface plots. Results showed that ANFIS prediction was 48% more accurate compared with that provided by the FFNN model.

Keywords Laser texturing · Artificial neural network · Adaptive neuro-fuzzy inference system

1 Introduction

Joining plays a significant role in manufacturing such as in automotive engineering for the assembly of parts and devices [1]. Mechanical joints for bonding parts in assembly lines can be joined via many different gluing options [2]. Press-fit or interference fit is commonly used such as in clinching joints, hinge joints, and for bonding shafts and bearings. Interference fits joints bond two components together by friction, often with a single quick stroke [3]. The creation of patterned surface microstructures on interference fit joints can be achieved in many ways, for example, abrasive blasting, reactive-ion

etching, and ultrasonic machining [2]. However, laser technology offers more control and precision over the produced geometry [3]. Laser surface texturing (LST) has been used for three decades in manufacturing industry for improvement and control of tribological characteristics of materials. However, the use of this process for press-fit joints has recently been developed [2]. LST on interference joint surfaces is a complex, stochastic process and a number of variables play a significant role in the process. Therefore, the development of an appropriate model which can approximate the effects of the most important features on the resulting geometry is of significant importance.

Several studies have been reported on the application of supervised machine learning methods for predicting the output of the laser process [4, 5]. Artificial neural network (ANN) and fuzzy logic have been applied successfully previously for prediction of some laser processes [4, 6]. Approximation methods which are related to artificial intelligence are secondary tools which use data generated through experiments for the estimation manufacturing process outputs [4]. Aminian et al. investigated the performance of ANN and applied

✉ H. Sohrabpoor
h.sohrab@outlook.com

¹ Advanced Processing Technology Research Centre, Dublin City University, Dublin, Ireland

² I-Form, Advanced Manufacturing Research Centre, Dublin City University, Dublin, Ireland

adaptive neuro-fuzzy system (ANFIS) on the laser machining and welding processes [5]. In their work, these authors noted that ANFIS was a better predictor compared with response surface methodology (RSM) and ANN. Biswas et al. used feedforward neural network (FFNN) for estimation of characterization of microdrilling on titanium nitride-alumina composite [6]. It was observed that an ANN node structure of 5-11-3 with 11 neurons in the hidden layer provided the least model error. Sohrabpoor et al. used ANFIS to predict laser powder deposition process outputs such as catchment efficiency and height [7]. Additionally, ANFIS was employed in selective laser sintering to correlate relationship between input parameters such as laser power and scan speed, and output factors including tensile strength and elongation [8]. The authors have also reported previously the use of ANFIS for laser processing and demonstrated the high capability and reliability of this model [9–12]. Pandremenos et al. used a mixture of neural network and design structure matrices for the link between clustering efficiency and interactions of products components [13]. They found that their especial algorithm is more efficient with the empirical one [13]. Karagiannis et al. applied feedforward back-propagation for approximation of yield surface magnitude in milling process [14]. They concluded that the model had an acceptable performance for correlation of inputs and results [14]. Also, some other studies have been carried out for the practicality of ANFIS and FFNN in the manufacturing process [15–18].

The experimental values are used to train a feedforward back-propagation artificial neural network for the prediction of the yield surface roughness magnitude.

Laser surface texturing of stainless-steel for interference fit is a novel technique developed by the co-authors. Interference fit is no more compliant pins that focused on joining technique; rather it has become an enabling technique for innovations in high-tech industries, such as safety-critical fueling applications. In the developed LST technique, the control of diameter increase is crucial to achieve different levels of fastening between the joining parts, and this control also determines the insertion and pull out forces. Therefore, in order to provide design flexibility, increasing strength and reliability of LST for interference fits, it is desirable to fully model the laser processing input parameters and use artificial intelligence techniques to predict the results.

In this study, investigations were performed for the first time and for the selection of best approach for the estimation of the characteristics of LST on 316L cylindrical pins for the interference fit joint. Although there are many factors which are related to the strength of the bonding, the most important parameters of diameter increase (DI), insertion force (IF), and removal force (RF) were studied. To achieve this goal, the actual data sets were extracted from the response surface methodology equations [3]. For the LST process, FFNN and ANFIS were applied

separately. The validity of the developed models was measured based on percentage error prediction (PEP). The effect of input parameters on each process outputs is analysed.

The interference fit has innovative applications in security-critical components in automobile and aerospace industry where a secure joint with high level of security, and reliability is required. Therefore, in order to determine the laser-processing parameters tailored for specific needs in terms of material, tightness level, applied and removal force, and reliability, artificial intelligence approaches can be further examined and investigated. The development of reliable and accurate artificial intelligent solutions is required that can predict most influencing processing parameters and provide solution to approximate the resulting properties as demonstrated previously using unsupervised and supervised learning methods.

Based on the literature review, no study has been carried out to demonstrate the difference between ANFIS and FFNN on LST. This comparison can be useful not only in modelling terms but also on practical perspective, and manufacturing industries can refer to this evaluation for the prediction of results which ensure quality of product, to reduce the manufacturing cost and to increase the quality of cold joints.

2 Methodology

2.1 Development of FFNN model

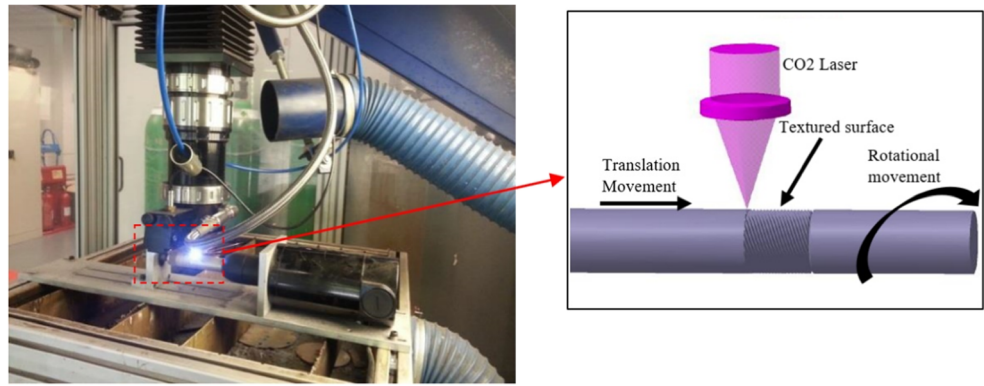
Neural network (NN) is a logical structure, in which multiple processing elements communicate with each other through the interconnections between the processors. The knowledge is presented by the interconnection weight, which is adjusted during the learning stage [13]. Backpropagation (BP) learning algorithm uses a gradient search technique to minimise the mean square between the actual output pattern of the network and the desired output pattern.

In FFNN, weights were fixed, and the activation function was examined and selected based on mean absolute error (MAE). More details were reported previously [4]. Like other approximation methods, FFNN was implemented including testing (20%) and training (80%), and MAE was utilised as the criteria of error in FFNN. The equation used for calculation of MAE is:

$$\text{MAE} = \frac{1}{T} \sum_{i=1}^T |t_i - a_i| \quad (1)$$

where T is the number of test data, t_i is the tested value, and a_i is the predicted value from ANFIS.

Fig. 1 Schematic of scanning process on an interference fit sample with CO₂ laser



2.2 Description of ANFIS

ANFIS is a machine-learning method with a mixture of NN and fuzzy logic for deriving the connections between the input and response elements [16]. The ANFIS model for this study was made of five layers each of which consists of some nodes. Like NN, in ANFIS, nodes transform from each layer to the next layer. The accuracy of trained data was examined by root mean square error (RMSE), the formula for which is:

$$\text{RMSE} = \sqrt{\frac{1}{M} \sum_{z=1}^M (S_z - Y_z)^2} \quad (2)$$

where M is the training value, S_z is actual response value, and Y_z is the model response value in training.

2.3 Materials

The data used for validation of the designed models was obtained from design of experiment (DoE) study on laser surface texturing for interference fit technique. This study was performed by the co-authors and reported previously [2, 19]. Briefly, cylindrical 316L stainless steel pins of 10 mm in diameter and 60-mm length were laser textured. The laser process as shown in Fig. 1 was carried out using a computerised numerical control (CNC) CO₂ laser, Rofin DC-015, with 1.5-kW maximum average power. The focal position was set at a distance of 1 mm below the sample surface to achieve 0.2-mm diameter focal spot size over the sample surface. Hub flanges of the same material were machined to 30-mm external diameter and centre-drilled and reamed to give the final hole

diameter of 10.05 ± 0.003 mm. Table 1 shows the input parameters including laser power (LP), pulse repetition frequency (PRF), and overlap (OL) between each laser scan and their levels which were used for experimental sample preparation. Laser power is the most important input parameter which determines the amount of thermal energy delivered to the sample being laser treated. The laser power was varied from 300 to 400 W and 500 W. In pulsed laser surface processing, the pulse repetition frequency determines the heat build-up between the pulses. The time interval between the laser pulses should be shorter than the thermal diffusivity of the material in order to build up amount of heat required for melting of the upper layer surface. Therefore, PRF was set at 100 Hz, 200 Hz, and 300 Hz, and the pulse width was set at 1.6 ms to examine the effect of PRF on the resulting surface properties of the laser processed samples. For interference fit application, precise control over micro-texture longitudinal and circumferential dimensions is required. To control the laser texture geometry, the laser scan overlap over the sample surface must be accurately controlled as multiple scanning of the same area will result in different surface texture. Three different overlap scenarios were studied including negative, positive, and zero overlaps to examine the effect on microstructure. The overlap was controlled by controlling the rotational and translational speeds of the sample such that the laser spots were overlapped to the same extent in the circumferential and longitudinal directions. Detailed mathematical relationships used to calculate overlap percentage for all three scenarios according to sample geometry, laser processing parameter (PRF), and rotational and longitudinal speeds have been reported previously [19].

For the current study, diameter increase (DI), insertion force (IF), and removal force (RF) were selected as output parameters from the previous study [2]. Details on methods used to obtain these results have been reported [2]. Briefly details on selection of these parameters for the current study and methodologies used to measure these parameters previously are as follows. The creation of microstructures on the surface of the laser processed stainless steel pins resulted in increased diameter. The change in the microstructure from austenite to large volume

Table 1 Laser surface texturing set DoE process factors and their levels

Process factors	Units	Symbols	Levels		
			-1	0	1
Laser power	W	LP	300	400	500
Pulse reputation frequency	Hz	PRF	100	200	300
Overlap	%	OV	-20	0	20

martensite phase also contributed to increased pin diameters [1, 2]. The diameter of the pin is directly related to the amount of interference. The control over diameter increase provides control over the tightness of the fit. Therefore, DI was selected as output parameter in this study. Diameters of the laser processed pins were measured by 0.05-mm resolution Vernier. Each measurement was taken 10 times, and average values were obtained. The ratio of insertion and pull out forces determines the efficiency of the interference fit. The reduction in insertion force makes the process economical and the removal force determines the tightness of the interference. Being the crucial factors determining the interference fit, IF and RF were selected as output parameters in the current study. The insertion and pull-out forces were measured using a Zwick Z-50 testing machine with the Zwick TestXpert simulation software. The insertion and pull-out tests were performed at speed of 5 mm/min (for further details, see [2]).

3 Results and discussion

The approximation methods including FFNN and ANFIS were used to approximate the output of the laser surface texturing of stainless-steel pins for interference fit application. In FFNN and ANFIS models, in order to increase the reliability and validity of the data, each run repeated three times, and average of them is reported.

3.1 Development of FFNN model

As the measured values of the three selected output parameters were largely different, the models were splitted into 4 networks to achieve maximum efficiency separately for each parameter.

3.1.1 K-fold cross-validation

In order to avoid overfitting and having lower bias, 4-fold cross-validation approach applied. Cross-validation is a re-sampling procedure used to evaluate machine learning models on a limited data sample [20]. In k-folds cross-validation, we split our data into k different subsets (or folds). We use k-1 subsets to train our data and leave the last subset (or the last fold) as test data. We then average the model against each of the folds and then finalise our model. After that, we test it against the test set. The procedure has a single parameter called k that refers to the number of groups that a given data sample is to be split into. As such, the procedure is often called k-fold cross-validation. When a specific value for k is chosen, it may be used in place of k in the reference to the model, which in this case, data is splitted to 4 folds (Fig. 2). For the cross-validation process, first we picked 4 separate learning experiments which included one testing test and remaining for training sets. This process is repeated 4 times, and finally we got the average test results from those experiments.

For developing the FFNN model, the initial step was training. Out of 27 datapoints available from the experiments performed previously [2], 21 datasets were selected arbitrary for training, and the remaining (6 datasets) were kept for testing the FFNN model (i.e. fold #1). In order to select the FFNN model which provides most accurate approximation, 9 training functions and 6 structures were tested. In hidden layers, the number of neurons should be higher than inputs. Therefore, the examination should be started from 4 neurons were selected for the first hidden. Minimum MAE was selected for each output. From Table 2, a network with 3-5-1 structure, for DI and IF, and 3-7-1 structure for RF are the modest accurate model due to lowest values of MAE. Figures 3, 4, and 5 present the comparison between the actual datasets and predicted datasets from the FFNN and ANFIS models fold #4

Fig. 2 Structure of cross validation for 4 folds

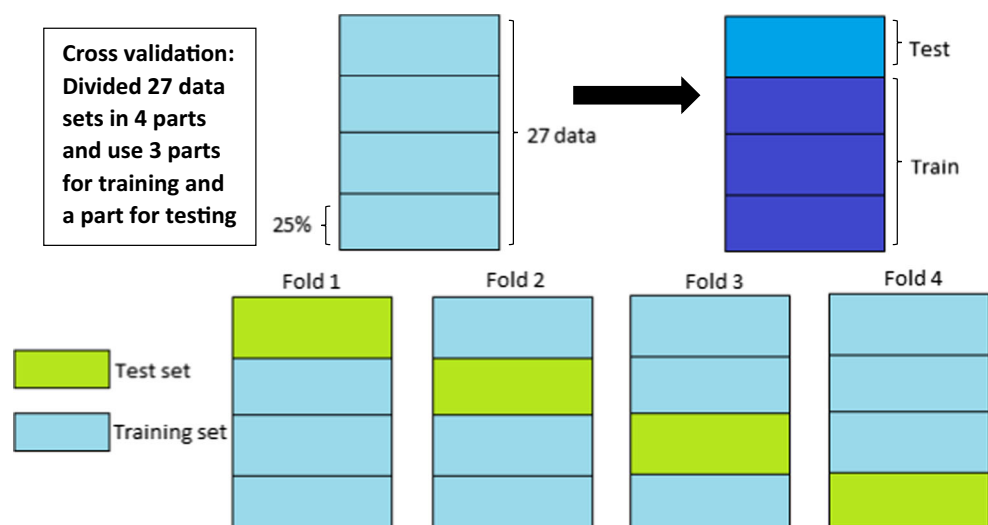


Table 2 Obtained MAE for various FFNN topographies under various training function

Outputs	Structure	Mean absolute error (MAE)				
		Fold #1	Fold #2	Fold #3	Fold #4	Average
DI	3-4-1	0.1214	0.1303	0.286	0.1709	0.1771
	3-5-1	0.102	0.1254	0.1903	0.1363	0.1391
	3-6-1	0.1768	0.1227	0.2207	0.2762	0.1991
	3-7-1	0.1359	0.259	0.2031	0.1053	0.1758
	3-8-1	0.245	0.2772	0.1729	0.1605	0.2139
	3-9-1	0.1446	0.2636	0.2039	0.1336	0.1864
IF	3-4-1	9.5422	7.681	11.8953	10.9615	10.02
	3-5-1	9.6862	6.4945	6.3013	14.3468	9.2072
	3-6-1	12.2945	6.3225	9.5408	10.4056	9.6408
	3-7-1	8.761	8.3664	12.3194	9.5307	9.7218
	3-8-1	9.5366	10.9437	13.0343	10.094	10.9021
	3-9-1	13.6917	9.2882	12.7691	10.2411	9.2475
RF	3-4-1	1.5413	1.4407	3.6875	3.3059	2.4935
	3-5-1	4.2451	2.541	2.6988	3.2035	3.1721
	3-6-1	2.5167	2.5392	2.7247	3.847	2.9069
	3-7-1	1.4931	2.8258	2.2417	3.9129	2.6183
	3-8-1	2.3913	2.325	3.28	3.0497	2.7615
	3-9-1	2.8758	2.6281	2.2546	3.1993	2.73945

(i.e. fold with highest MAEs). As can be seen from these figures, the optimised models predicted well with the actual experimental recorded data (Table 3).

3.2 Development of ANFIS model

For the approximation of the results with ANFIS for the LST process, like FFNN, testing and training datasets need to be selected. Testing and training datasets from the FFNN model were selected for ANFIS model. In this way, a direct comparison between the models could be performed. To implement cross-validation on modelling of DI, IF and RF, four data sets

were identified (based on Fig. 2). For choosing the best and most accurate model, the structure of ANFIS was varied and different structures such as 3-3-3-3 and 4-4-4-4 were examined. It was observed that a 2-2-2 model with 200 epochs and Sugeno type of fuzzy-based rule had the lowest RMSE. Also, 8 membership functions (MF) in the ANFIS model were examined for finding the most appropriate model. It was found that triangular type of MF for diameter increase and insertion force and for removal, force trapezoid type of MF were the most accurate MF. Figures 6, 7, and 8 present comparison of the predicted values from the ANFIS and FFNN models with the actual data. It can be observed from the figures that the predicted data extremely well fitted with the measured data recorded from the experiments.

3.3 Calculation of correlation coefficient percentage

Correlation coefficient is a vital aspect used in statistics to calculate the strength and direction of the linear relationship or the statistical relationship (correlation) between the two population data sets [21]. This coefficient calculated based on the relation of FFNN and ANFIS test data to measured data in Figs. 4, 5, and 6 separately. This formula is defined as:

$$r_{x,y} = \frac{\sum_{i=1}^n (x_i - \bar{x})(y_i - \bar{y})}{\sum_{i=1}^n \sqrt{(x_i - \bar{x})^2} \sqrt{(y_i - \bar{y})^2}} \quad (3)$$

where n is sample size (here is 7), x_i and y_i are measured data points and predicted by ANFIS or FFNN, and \bar{x} is $\frac{1}{n} \sum_{i=1}^n x_i$ and analogously for \bar{y} . Table 4 shows the result of calculation of correlation coefficient. As Table 4 shows, ANFIS predicted significantly better compared with FFNN. Therefore, ANFIS selected as a final model for investigation of effect of each parameter on outputs.

Fig. 3 Comparison of measured, 3–5-1 FFNN and ANFIS values of testing data for DI for fold #4

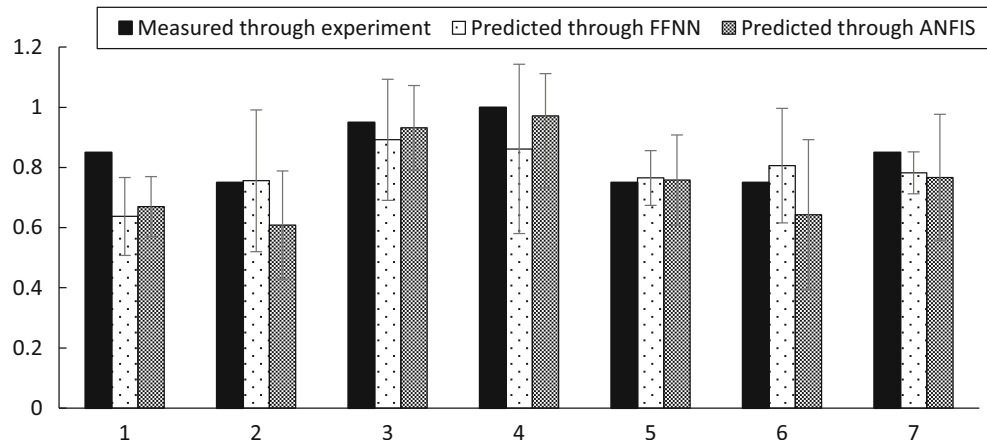
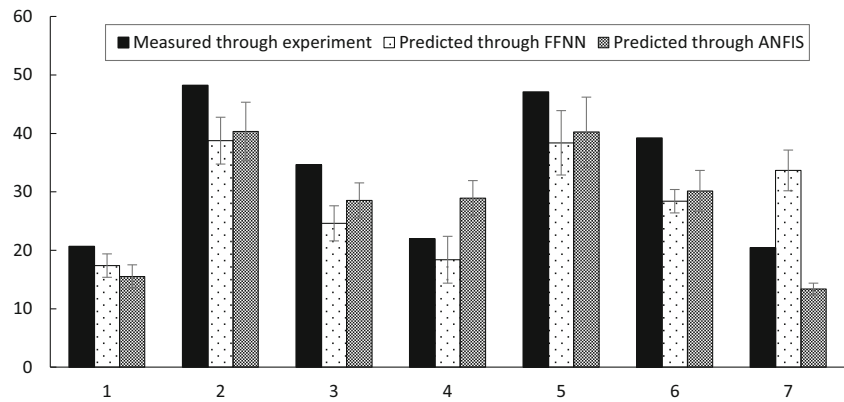


Fig. 4 Comparison of measured, 3–5-1 FFNN and ANFIS values of testing data for DI for fold #4



3.4 Comparison accuracies of developed models ANFIS and ANN

To compare the prediction accuracies of the developed model, the prediction error percentage (PEP) was measured and defined as follows:

$$PEP = \frac{1}{27} \sum_{i=1}^n \frac{|a_i - y_i|}{a_i} \quad (4)$$

where a_i is the actual data and y_i is the approximated data by the developed FFNN and ANFIS models. Figs. 6, 7, and 8 show the PEP values from ANFIS and FFNN which were calculated for DI, IF, and RF, respectively. It can be observed that ANFIS predicted more accurately the results compared to FFNN. These results are summarised in Table 3. Table 3 shows the overall comparison of PEP between the two models. As can be seen from Table 3, ANFIS improved the PEP more than 45%. These results show that the ANFIS model was more reliable and resilient to noise compared with FFNN. Hence, it can be suggested that ANFIS can predict the LST process more accurately and could serve as a precise machine learning method for the LST process (Table 5).

3.5 Analysis of responses: diameter increase, insertion force, and removal force

As observed from the results, ANFIS proved to be a more accurate model for prediction of DI, IF, and RF. Hence, the developed ANFIS model was used for analyzing in more detail the effects of laser surface-texturing process parameters on the responses. The 3D plots of ANFIS prediction surfaces were constructed, and the parameter effects were analysed, see Fig. 9.

From Fig. 9a, the highest values of DI were obtained when the PRF was low. Due to an increased heating time (from lower PRF), a larger amount of energy was input to the surface, and consequently a larger melt pool was produced, in turn, resulting in a higher DI. On the other hand, by increasing the laser power from 300 to 400 W, sufficient melting should occur. However, a further increase of the power from 400 to 500 W could cause over-melting and a loss of the material due to centrifugal forces, which could lead to a reduction in DI.

Based on the results shown in Fig. 9b, for positive values of OV% the DI will be considerably lowered due to over-melting. By comparing Fig. 9a and b, it seems that when the power and OV% were minimum and negative, respectively, and over-melting occurs, then a higher value of DI can be obtained, and there is an optimum range of PRF between 140 and 220 Hz.

Fig. 5 Comparison of measured, 3–7-1 FFNN and ANFIS values of testing data for RF for fold #4

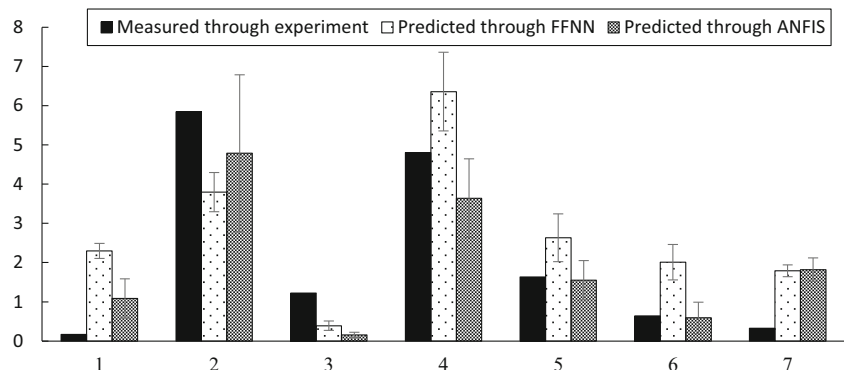


Table 3 Obtained RMSE for various ANFIS topographies under various training function

Output	Structure	Root mean square error (RMSE)				
		Fold #1	Fold #2	Fold #3	Fold #4	Average
DI	Triangular	0.12436	0.11419	0.10628	0.112	0.1142
	Trapezoid	0.18483	0.4081	0.1834	0.1598	0.2325
	Generalised bell	0.14131	0.3682	0.2551	0.2551	0.2549
	Gaussian	0.14004	0.3845	0.2528	0.5851	0.3407
	Pi shaped	0.1732	0.4866	0.2722	0.2972	0.2972
	Di sigmoidal	0.25378	0.5035	0.2972	0.2597	0.3285
IF	Triangular	6.9956	5.05	6.469	11.3502	7.4662
	Trapezoid	25.2873	5.9037	7.469	13.2208	12.9702
	Generalised bell	13.7131	5.7618	13.64	13.5973	11.6780
	Gaussian	13.0184	12.1689	7.66	14.237	11.71
	Pi shaped	25.2873	5.7916	7.466	13.745	13.72
	Di sigmoidal	25.1845	5.7454	7.469	14.1162	13.1287
RF	Triangular	7.788	4.701	4.701	4.8747	5.5391
	Trapezoid	3.8171	2.6461	1.6461	2.2684	2.59322
	Generalised bell	7.7969	4.831	4.8431	5.3683	4.9598
	Gaussian	7.7831	4.7128	4.7128	4.2635	5.518
	Pi shaped	7.8219	4.8796	4.8796	5.0876	5.6637
	Di sigmoidal	7.8141	4.9152	4.9151	5.4665	5.7777

Fig. 6 PEP modeling of diameter increases by ANFIS and FFNN

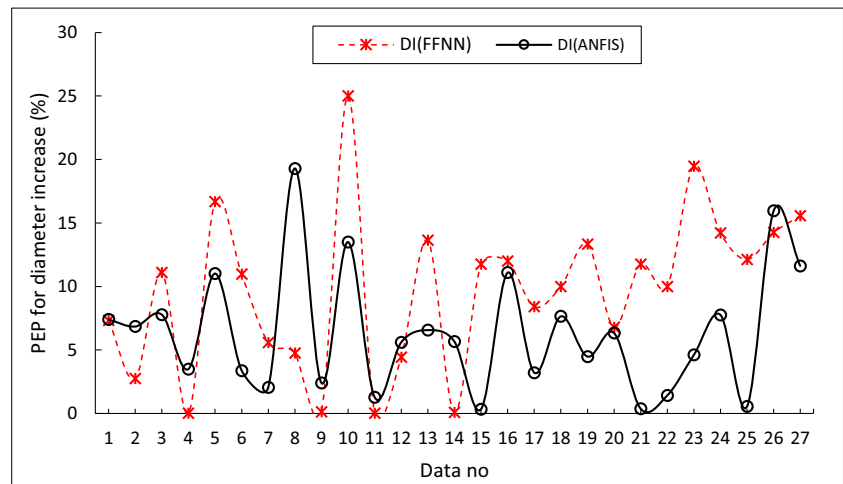


Fig. 7 PEP modeling of insertion force by ANFIS and FFNN

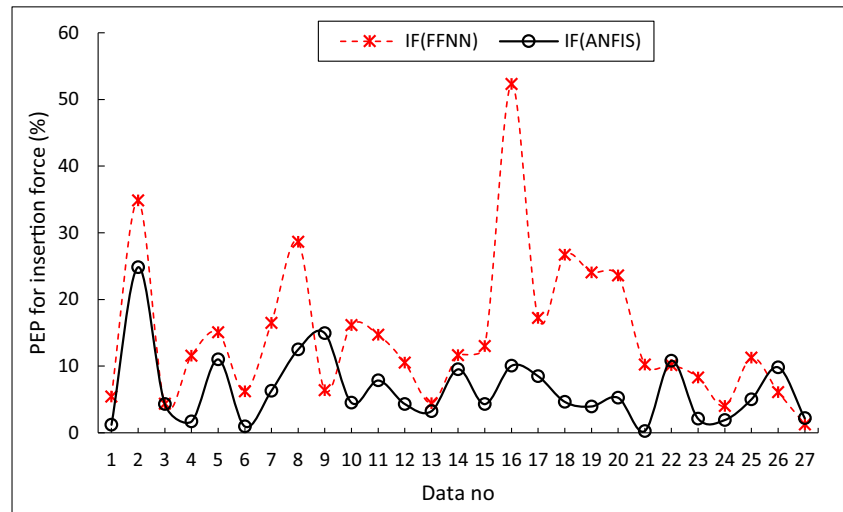


Fig. 8 PEP modeling of removal force by ANFIS and FFNN

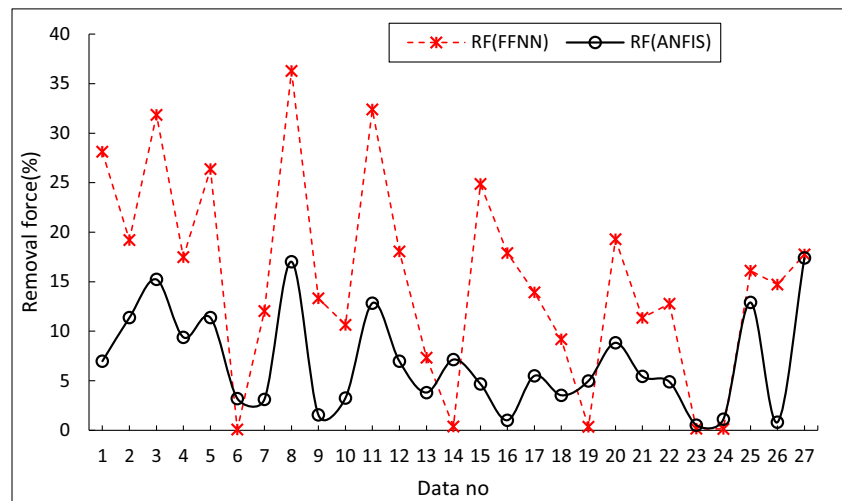


Figure 9c and d show the response plots of IF values obtained at various ranges of power, PRF, and OV%. Both of the plots indicated that enhancing the amount of PRF will lead to a sharp decrease in IF. In fact, when the PRF is increased, due to the fast heating and cooling steps, the amount of residual stresses can be increased that may cause the formation of a brittle surface, lowering the resistance of the material under the insertion force. On the other hand, when the PRF is low, then the possibility of austenite-martensitic phase transformation occurrence will be increased, resulting in a surface hardening of the material and a higher insertion force. Therefore, by a suitable heat-treatment process during laser movement, a higher bond strength, gripping, insertion, and removal force can be provided. Figure 9d demonstrates that positive values of OV% could sharply reduce the bond strength. This could be due to the re-melting and overheating that could deteriorate the formation of martensitic phase. Also, these phase transformations are known to be sensitive to the heating/cooling cycle time and temperature.

Figure 9e and f demonstrate the variation of RF for tested input PRF, power, and OV%. Almost, the same trend for the IF was obtained for the RF in case of power and overlap. From the bond strength point of view for having a suitable cold joint, it can be concluded that at high laser powers which brings a high thermal energy, a strong bond can be obtained if the OV% is negative and the PRF value is lower than 220 Hz, where suitable conditions for martensitic phase formation would be obtained.

Table 4 Correlation coefficient for outputs

Outputs	FFNN (%)	ANFIS (%)
DI	62.12	88.62
IF	72.5	89.7
RF	75.2	90.56

4 Conclusion and future perspectives

This research dealt with the simulation and approximation of diameter increase, insertion force, and removal force for laser surface-textured 316L interference fit joints with two supervised learning approaches. For finding the effect of a mixture of inputs on the responses, two models FFNN and ANFIS were used. However, to determine the accuracy of the developed models, different error parameters were examined for a variety of model structures. By testing and training of various FFNN, 3-5-1 structure for DI and IF and 3-7-1 structure for RF are selected. The selection of the structures was made on the basis of the lowest value of MAE. ANFIS 2-2-2 structure with Gaussian2 MF and backpropagation optimization, D sigmoidal MF and hybrid, and Pi-shaped MF showed the lowest RMSEs for DI, IF, and RF, respectively. The ANFIS model produces lower values of PEP compared with FFNN. Hence, it was selected as the most powerful simulation for approximation and analysis of the responses. The effect of each processing parameters (based on interaction terms) was investigated by using response surfaces which were plotted based on the ANFIS model. With suitable laser processing parameters, higher gripping insertion and removal forces can be provided and at higher laser powers, where the OV% is negative, and for PRF values lower than 220 Hz. The ANFIS has some advantages over FFNN, including the ability to capture the nonlinear structure of a process, adaptation capability, and rapid learning capacity. ANFIS uses either backpropagation or a combination of least squares estimation and

Table 5 Comparison between ANFIS and FFNN for all outputs

Modelling type	DI	IF	RF	Overall PEP
FFNN	0.097139	0.146085	0.152609	0.395833
ANFIS	0.063594	0.065152	0.068435	0.203181

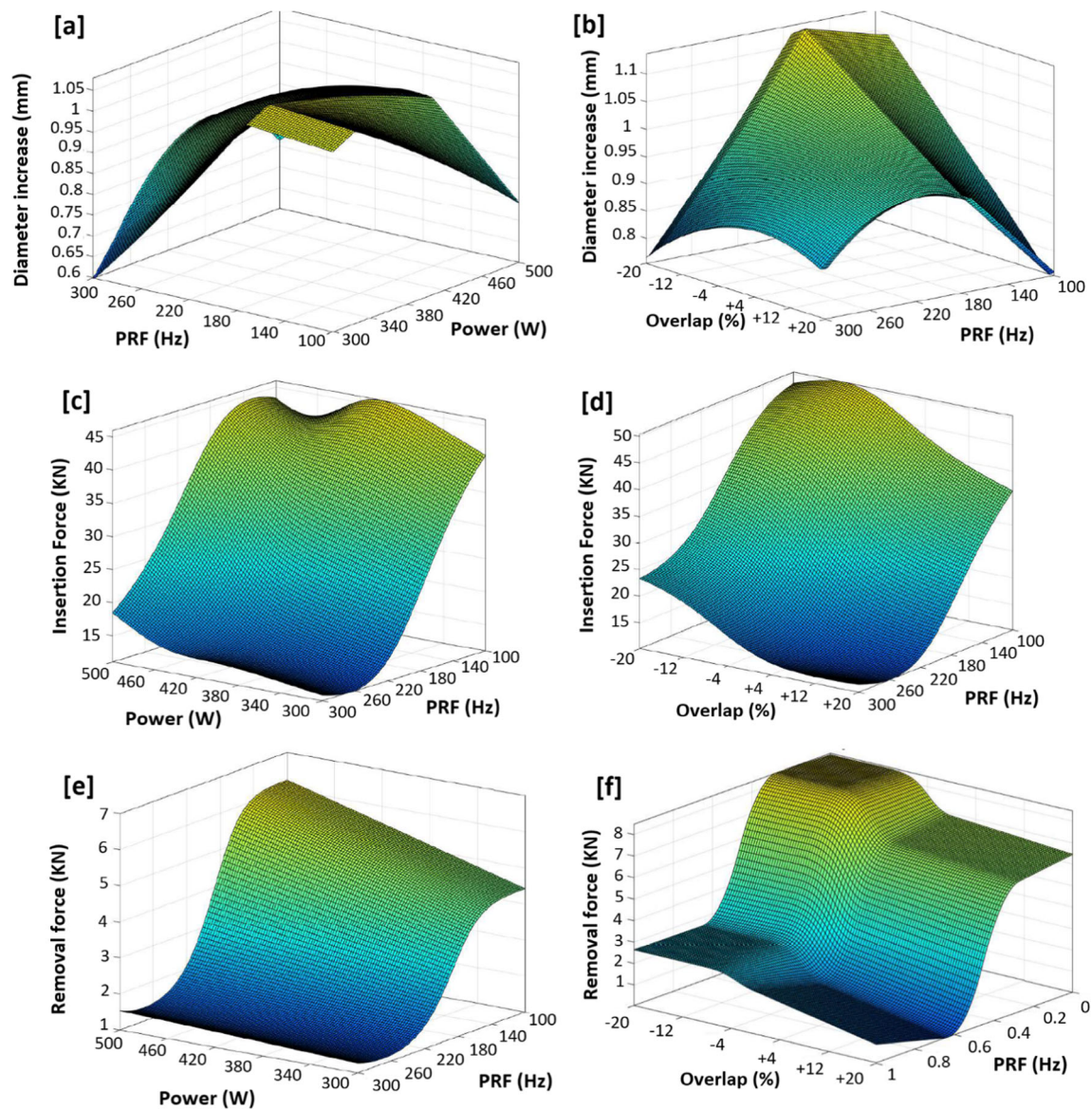


Fig. 9 Surface plots of diameter increase versus process inputs (a and b), insertion force versus process inputs (c and d), and removal force versus process inputs (e and f)

backpropagation for membership function parameter estimation. ANFIS algorithm has a hybrid learning approaches in its structure. Thus, ANFIS has the advantage to combine both ANN and fuzzy knowledge. So ANFIS is more precise in term of prediction. Due to the fact that the laser surface texturing processing technologies are really high-cost process, the developing model can give a vision regarding the selection of best process parameters without needing a high number of experiments. Otherwise stated, to reach desirable performance in each process, the developed model is beneficial to select optimal parameters without conducting extensive experiments, and it has a strong economic justification.

Since ANFIS has proven a good tool for approximation of results, ANFIS model can be applied as objective function to select optimal parameters of manufacturing process, in which

the process reaches to its desirable mechanical properties by using the metaheuristic algorithms such as simulated annealing algorithm and bee colony.

Funding information This research is supported by a research grant from the Science Foundation Ireland (SFI) under Grant Number 16/RC/3872 and is co-funded under the European Regional Development Fund and by I-Form industry partners. This work is also supported by Irish Research Council Government of Ireland Scholarship.

References

1. Murcinkova Z, Baron P, Pollak M (2018) Study of the press fit bearing-shaft joint dimensional parameters by analytical and numerical approach. *Adv Mater Sci Eng*

2. Obeidi M, McCarthy E, Kailas L, Brabazon D (2018) Laser surface texturing of stainless steel 316L cylindrical pins for interference fit applications. *J Mater Process Technol* 252:58–68
3. Hüyük H, Music O, Koç A, Kardogan C, Bayram C (2014) Analysis of elastic-plastic interference-fit joints. *Procedia Engineering* 81:2030–2035
4. H. Sohrabpoor, A. Issa, A. Hamaoy, I. Ahad, E. Chikarakara, K. Bagga, D. Brabazon, Development of laser processing technologies via experimental design, Chapter 24, pp. 707–730, 2nd edn, 2017
5. Aminian M, Teimouri R (2015) Application of soft computing techniques for modeling and analysis of MRR and taper in laser machining process as well as weld strength and weld width in laser welding process. *Soft Comput* 19:793–810
6. Biswas A, Rajat S, Gupta R (2018) Application of artificial neural network for performance evaluation of vertical axis wind turbine rotor. *Int J Ambient Energy* 37(2):1–10
7. sohrabpoor H (2016) Analysis of laser powder deposition parameters: ANFIS modeling and ICA optimization. *Optik* 127(8):4031–4038
8. Sohrabpoor H, Negi S, Shaiesteh H, Ahad IU, Brabazon D (2018) Optimizing selective laser sintering process by grey relational analysis and soft computing techniques. *Optik* 174:185–194
9. Umrao R, Sharma L, Singh R, Singh T (2018) Determination of strength and modulus of elasticity of heterogenous sedimentary rocks: An ANFIS predictive technique. *Measurement* 126:194–201
10. Teimouri R, Shrabpoor H (2013) Application of adaptive neuro-fuzzy inference system and cuckoo optimization algorithm for analyzing electro chemical machining process. *Front Mech Eng* 8(4): 429–442
11. Gholami A, Bonakdari H, Ebtehaj I, Mohammadi M, Gharabaghi B, Khodashenase S (2018) Uncertainty analysis of intelligent model of hybrid genetic algorithm and particle swarm optimization with ANFIS to predict threshold bank profile shape based on digital laser approach sensing. *Measurement* 121:294–303
12. Fister I, Perc M, Kamal S, Fister I (2015) A review of chaos-based firefly algorithms: Perspectives and research challenges. *Appl Math Comput* 252(1):155–165
13. Pandremenos J, Chrysosolouris G (2011) A neural network approach for the development of modular product architectures. *Int J Comput Integr Manuf* 24(10):879–887
14. Karagiannis S, Stavropoulos P, Ziogas C, Kechagias J (2013) Prediction of surface roughness magnitude in computer numerical controlled end milling processes using neural networks, by considering a set of influence parameters: an aluminium alloy 5083 case study. *Proc Inst Mech Eng B J Eng Manuf* 228(2):233–244
15. Ojha V, Abraham A, Snášel V (2017) Metaheuristic design of feedforward neural networks: a review of two decades of research. *Eng Appl Artif Intell* 60:97–116
16. Baseri H, Damirchi H (2011) Rediction of the ferrite-Core probe performance using a neural network approach. *Mater Manuf Process*
17. Shamsipour M, Pahlevani Z, Ostad M, Mazahery S (2016) Optimization of the EMS process parameters in compocasting of high-wear-resistant Al-nano-TiC composites. *Appl Phys A* 122
18. Acı M (2016) Artificial neural network approach for atomic coordinate prediction of carbon nanotubes. *Appl Phys A* 122
19. Obeidi MA, McCarthy E, Brabazon D (2016) Methodology of laser processing for precise control of surface micro-topology. *Surf Coat Technol* 307(Part A)
20. Tsamardinos I, Greasidou E, Borboudakis G (2018) Bootstrapping the out-of-sample predictions for efficient and accurate cross-validation. *Mach Learn* 107(12):1895–1922
21. Yurdakul M, Tansel İÇ Y (2009) Application of correlation test to criteria selection for multi criteria decision making (MCDM) models. *Int J Adv Manuf Technol* 40:403–412

Publisher's note Springer Nature remains neutral with regard to jurisdictional claims in published maps and institutional affiliations.